

Video Article

# The Arteriovenous (AV) Loop in a Small Animal Model to Study Angiogenesis and Vascularized Tissue Engineering

Annika Weigand<sup>1</sup>, Justus P. Beier<sup>1</sup>, Andreas Arkudas<sup>1</sup>, Majida Al-Abboodi<sup>1,2</sup>, Elias Polykandriotis<sup>3</sup>, Raymund E. Horch<sup>1</sup>, Anja M. Boos<sup>1</sup>

<sup>1</sup>Department of Plastic and Hand Surgery and Laboratory for Tissue Engineering and Regenerative Medicine, University Hospital of Erlangen, Friedrich-Alexander University of Erlangen-Nürnberg (FAU)

<sup>2</sup>Genetic Engineering and Biotechnology Institute for Postgraduate Studies, Baghdad University

<sup>3</sup>Department of Plastic, Hand and Microsurgery, Sana Klinikum Hof GmbH

Correspondence to: Annika Weigand at [annika.weigand@uk-erlangen.de](mailto:annika.weigand@uk-erlangen.de)

URL: <https://www.jove.com/video/54676>

DOI: [doi:10.3791/54676](https://doi.org/10.3791/54676)

Keywords: Bioengineering, Issue 117, arteriovenous loop, angiogenesis, vasculogenesis, microsurgery, animal model, tissue engineering, regenerative medicine, biomedical engineering

Date Published: 11/2/2016

Citation: Weigand, A., Beier, J.P., Arkudas, A., Al-Abboodi, M., Polykandriotis, E., Horch, R.E., Boos, A.M. The Arteriovenous (AV) Loop in a Small Animal Model to Study Angiogenesis and Vascularized Tissue Engineering. *J. Vis. Exp.* (117), e54676, doi:10.3791/54676 (2016).

## Abstract

A functional blood vessel network is a prerequisite for the survival and growth of almost all tissues and organs in the human body. Moreover, in pathological situations such as cancer, vascularization plays a leading role in disease progression. Consequently, there is a strong need for a standardized and well-characterized *in vivo* model in order to elucidate the mechanisms of neovascularization and develop different vascularization approaches for tissue engineering and regenerative medicine.

We describe a microsurgical approach for a small animal model for induction of a vascular axis consisting of a vein and artery that are anastomosed to an arteriovenous (AV) loop. The AV loop is transferred to an enclosed implantation chamber to create an isolated microenvironment *in vivo*, which is connected to the living organism only by means of the vascular axis. Using 3D imaging (MRI, micro-CT) and immunohistology, the growing vasculature can be visualized over time. By implanting different cells, growth factors and matrices, their function in blood vessel network formation can be analyzed without any disturbing influences from the surroundings in a well controllable environment.

In addition to angiogenesis and antiangiogenesis studies, the AV loop model is also perfectly suited for engineering vascularized tissues. After a certain prevascularization time, the generated tissues can be transplanted into the defect site and microsurgically connected to the local vessels, thereby ensuring immediate blood supply and integration of the engineered tissue. By varying the matrices, cells, growth factors and chamber architecture, it is possible to generate various tissues, which can then be tailored to the individual patient's needs.

## Video Link

The video component of this article can be found at <https://www.jove.com/video/54676/>

## Introduction

Most tissues and organs in the human body are dependent on a functional blood vessel network that supplies nutrients, exchanges gases and removes waste products. Malfunction of this system caused by local or systemic vascular problems can lead to a multitude of severe diseases. Moreover, in research areas such as tissue engineering or regenerative medicine, a functional blood vessel network within artificially generated tissues or transplanted organs is indispensable for successful clinical application.

For decades researchers have been investigating the exact mechanisms involved in the growing vasculature to gain deeper insight into pathological situations in order to find novel therapeutic interventions and provide better prevention of vascular disorders. In the first step, basic processes such as cell-cell interactions or the effect of molecules on cells of the vascular system are usually investigated by *in vitro* 2D or 3D experiments. Traditional 2D models are easy to perform, are well established and have contributed greatly to a better understanding of these processes. For the first time in 1980, Folkman *et al.* reported *in vitro* angiogenesis seeding of capillary endothelial cells on gelatin coated plates<sup>1</sup>. This immediately gave way to publication of a multitude of further 2D angiogenesis experiments on endothelial cell tube formation assay<sup>2</sup>, migration assay<sup>3</sup> and the co-culturing of different cell types<sup>4</sup>, as well as others. These assays are still used today and accepted as standard *in vitro* methods.

However, this experimental setup is not always appropriate for the study of *in vivo* cell behavior since most cell types require a 3D environment to form relevant physiological tissue structures<sup>5</sup>. It could be shown that the architecture of the 3D matrix is decisive for capillary morphogenesis<sup>6</sup> and that cell-extra cellular matrix (ECM) interactions and 3D culture conditions regulate important factors involved in tumor angiogenesis<sup>7</sup>. The 3D matrix provides complex mechanical inputs, can bind effector proteins and establish tissue-scale solute concentration gradients. Moreover, it is considered necessary in order to imitate *in vivo* morphogenetic and remodeling steps in complex tissues<sup>5</sup>. In these systems, both angiogenesis and vasculogenesis can be studied. While angiogenesis describes the sprouting of capillaries from preexisting blood vessels<sup>8</sup>,

vasculogenesis refers to the *de novo* formation of blood vessels through endothelial cells or their progenitors<sup>9,10</sup>. Maturation of vessels is described in a process called 'arteriogenesis' via recruitment of smooth muscle cells<sup>11</sup>. A typical angiogenic *in vitro* model is the sprouting of endothelial cells from existing monolayers seeded as a monolayer on gel surfaces, on surface of microspheres embedded within a gel or by building endothelial cell spheroids<sup>12</sup>. In vasculogenic models single endothelial cells are entrapped in a 3D gel. They interact with adjacent endothelial cells to form vascular structures and networks *de novo*, typically in combination with supportive cells<sup>12</sup>.

However, even complex 3D *in vitro* models cannot mimic *in vivo* settings completely given the multitude of cell-cell and cell-ECM interactions<sup>13</sup>. Substances with high *in vitro* activity do not automatically show the same effects *in vivo* and *vice versa*<sup>14</sup>. For a comprehensive analysis of vascularization processes there is an urgent need to develop *in vivo* models that better simulate the situation in the body. A large range of *in vivo* angiogenesis assays are described in the literature, including the chick chorioallantoic membrane assay (CAM), the zebrafish model, the corneal angiogenesis assay, the dorsal air sac model, the dorsal skinfold chamber, the subcutaneous tumor models<sup>14</sup>. However, these assays are often associated with limitations, such as rapid morphological changes, problems in distinguishing new capillaries from already existing ones in the CAM assay, or the limited space in the corneal angiogenesis assay<sup>15</sup>. Furthermore, non-mammalian systems are used (e.g., the zebrafish model<sup>16</sup>), which leads to problems in xenotransplantation<sup>17</sup>. In the subcutaneous tumor model, angiogenesis originating only from the tumor itself cannot be analyzed since the adjacent tissue greatly contributes to the vascularization process. Moreover, the surrounding tissue can have a decisive role in shaping the tumor microenvironment<sup>18</sup>.

Not only for studying angiogenesis or vasculogenesis is there a strong need for a standardized and well-characterized *in vivo* model but also for studying different vascularization strategies in tissue engineering and regenerative medicine. Today, the generation of complex artificial organs or tissues is possible both *in vitro* and *in vivo*. 3D bioprinting provides an on-demand fabrication technique for generating complex 3D functional living tissues<sup>19</sup>. Furthermore, bioreactors can be used for generating tissues<sup>20</sup> or even the own body can be used as bioreactor<sup>21</sup>. However, the main barrier to successful application of artificially generated tissues is the lack of vascularization within the engineered constructs. Immediate connection to the host's vasculature after transplantation is a major prerequisite for survival, especially in the case of large-scale artificial tissues or organs.

Different *in vitro* or *in vivo* prevascularization strategies were developed to establish a functional microvasculature in constructs prior to implantation<sup>22</sup>. The implantation of a scaffold with *in vitro* preformed engineered capillaries onto the dorsal skin of mice led to rapid anastomosis of the mice vasculature within a day<sup>23</sup>. In contrast, a spheroid co-culture consisting of human mesenchymal stem cells and human umbilical vein endothelial cells assembled into a three-dimensional prevascular network developed further after *in vivo* implantation. However, anastomosis with the host vasculature was limited<sup>24</sup>. Above all, in poorly vascularized defects, such as necrotic or irradiated areas, this so-called extrinsic vascularization — the ingrowth of vessels from the surrounding area into the scaffold — often fails. Intrinsic vascularization, on the other hand, is based on a vascular axis as a source of new capillaries sprouting into the scaffold<sup>25</sup>. Using the axial vascularization approach, the engineered tissue can be transplanted with its vascular axis and connected to local vessels at the recipient site. Immediately after transplantation, the tissue is adequately supported by oxygen and nutrients, which creates the right conditions for optimal integration.

Due to the limited availability of models for investigating *in vivo* angiogenesis and in recognition of the growing importance of generating axially vascularized tissue, we developed the microsurgical approach of Erol and Spira further to generate an arteriovenous (AV) loop in the animal model<sup>26</sup>. The use of a completely closed implantation chamber makes this method very well suited to study blood vessel formation under "controlled", well characterized *in vivo* conditions (**Figure 1**). This model is not only useful for the investigation of angiogenesis but is also optimally suited for the axial vascularization of scaffolds for tissue engineering purposes.

## Protocol

The Animal Care Committee of the Friedrich-Alexander University of Erlangen-Nürnberg (FAU) and the Government of Middle Franconia, Germany, approved all the experiments. For the experiments, male Lewis rats with a body weight of 300 - 350 g were used.

## 1. The Arteriovenous Loop Model in the Rat

### 1. Implantation Procedure (Figure 2)

1. For anesthesia use a special plastic box that is connected *via* tube to the isoflurane vaporizer and closed by a lid. Turn on supply gas and flow meter between 0.8 - 1.5 L/min.
2. Place the rat in the induction plastic box and seal the top. Turn on isoflurane vaporizer to 5%.
3. Carefully observe the rat during induction of anesthesia. After 3 - 4 min, the rat will be anesthetized.
4. Confirm proper anesthesia: loss of righting reflex, loss of palpebral reflex, withdrawal reflex, positive corneal reflex.
5. Remove the rat from the box and check its weight for calculation of drugs. Apply eye ointment to prevent dryness while under anesthesia.
6. Administer pain medication and antibiotics (e.g., 7.5 mg/kg enrofloxacin subcutaneously (s. c.), 12.5 mg/kg tramadol and 100 mg/kg metamizole both intravenously (i. v.)). Administer weight-adapted crystalloids during operation (e.g., 30 ml/kg s. c.).
7. Place the rat on its back on a warming plate at 37 °C under anesthesia with 1 - 2% isoflurane inhalation administered *via* mask.
8. Monitor anesthesia properly and increase isoflurane if anesthesia level is too low (movement of the rat, response to pain, jaw tone, no loss of reflexes (see 1.1.4.), heart rate increasing). Be careful not to overdose isoflurane (loss of corneal reflexes, high heart rate, decrease in oxygen saturation). Use a special pulse oximetry for small animals for checking the oxygen saturation (95 - 100%) and heart rate (250 - 450/min) of the rat. During the operation monitor temperature of the rat (36 - 40 °C) and adjust temperature of the warming plate if necessary.
9. Shave the inner sides of the hind limbs with an electric razor and disinfect the area with antiseptics. Spread the hind limbs and fix them with adhesive tape.
10. Lay the rat under a surgical microscope and cover the rat with sterile draping. Ensure that the whole operation procedure is performed under sterile conditions.
11. Open the skin in the middle of the left thigh with a longitudinal incision from the upper knee to the groin using a scalpel (No. 10).

12. Cut the subcutaneous tissue and fascia in layers of approximately 3 cm in length using dissecting scissors and microforceps until the femoral vascular bundle is exposed from the pelvic artery in the groin to the bifurcation of the femoral artery in the knee.
13. Separate the vessels and remove the adventitia using adventitia scissors and microforceps.
14. Coagulate the side branches using electric coagulation. Cover the operation field with a damp compress.
15. Open the skin on the right side as described for the left side, 1.1.11 - 1.1.14.
16. For harvesting the venous graft, ligate the right femoral vein by electric coagulation on the proximal and distal ends at a distance of 1 - 1.5 cm.
17. Remove the venous graft with microforceps and flush the venous graft with a heparin solution (50 IU/ml in 0.9% sodium chloride solution) using an irrigation cannula and transfer it to the left thigh. Cover the operation field at the right side with a damp compress.
18. Ligate the femoral vein on the left side proximally at the inguinal region with a microvessel clamp. Coagulate the femoral vein distally by electric coagulation, at the upper knee before branching, at a distance of about 2 cm.
19. For anastomosis connect the proximal end of the venous graft with the proximal end of the vein by end-to-end anastomosis with an 11-0 suture. Use about 8 interrupted sutures. Begin with placing the first two sutures at the 12 o'clock and 6 o'clock positions. Then, put in 2 to 3 more sutures between these points on the front side and then put 2 to 3 more sutures into the back side.
20. Ligate the femoral artery in the same way described for the femoral vein (1.1.18.). Make sure the loop vessels are not twisted. Anastomose the distal end of the venous graft with the proximal end of the artery as described for the femoral vein (steps 1.1.19.).
21. Administer 25 IU heparin intravenously. Make again sure the loop vessels are not twisted, Remove the clamps and check for leakage and patency of the loop for about 5 min.
22. Dribble papaverine (e.g., 4 mg/ml) on the vessels to prevent vascular spasms. If there is patency, the loop expands and the pulse of the artery can be observed.
23. Prefill the implantation chamber with the first half (about 500  $\mu$ l) of the matrix (e.g., a hydrogel or a bone matrix with or without cells). Embed the loop into the implantation chamber.
24. Fill the implantation chamber with the second half of the matrix to a total volume of 1,000  $\mu$ l. Seal the chamber with the chamber lid.
25. Fix the implantation chamber on the thigh with a non-absorbable 6-0 suture. Fix the chamber lid with a non-absorbable 6-0 suture. Stop possible bleeding with electric coagulation.
26. Close the skin with absorbable 4-0 sutures. Cover the wound with aluminum spray.
27. Administer antibiotics and analgesics (e.g., 7.5 mg/kg enrofloxacin s. c., tramadol 12.5 mg/kg per os (p. o.) (through drinking water) for 3 - 5 days and afterwards depending on the behavior of the rat).
28. Turn the vaporizer off and allow the rat to breathe supply gas until it begins to awaken.
29. Place the rat in a box with thermal support and observe it carefully until fully recovered.
30. Do not leave the rat unattended until it has regained sufficient consciousness to maintain sternal recumbency.
31. Do not return the rat to the company of other animals until fully recovered.

## 2. Explantation Procedure

1. Perform the explantation after a short-time or long-time implantation (according to the study design, for examples please see References 27-32). Anesthetize the rat according to steps 1.1.1.-1.1.9.
2. Open the skin of the abdomen with a scalpel (No. 10) and move the intestines aside with a compress. Expose the abdominal aorta and the vena cava caudalis using cotton swabs.
3. Cannulate the abdominal aorta (e.g., 24 gauge plastic cannula) and cut the vena cava caudalis with dissecting scissors.
4. Flush the abdominal aorta with 0.9% sodium chloride solution containing 100 IU/ml heparin until the leaking fluid is clear. Perfuse the aorta with 30 ml perfusion solution (e.g., contrast agent or India ink).
5. Euthanize the rat by injection of a lethal dose of embutramide, mebezonium iodide, tetracaine hydrochloride injectable solution (0.1 - 0.2 ml/kg) in deep anesthesia.
6. Ligate the abdominal aorta and vena cava caudalis with a non-absorbable 4-0 suture.
7. Close the open wound area with 1 - 2 clamps. Store the rat for 24 hr at 4 °C (curing of the perfusion solution).
8. Place the rat on its back. Spread the hind limbs and fix them with adhesive tape.
9. Open the skin above the chamber with a longitudinal incision with a scalpel (No. 10).
10. Remove the connective tissue from the chamber and the loop pedicle using dissecting scissors and microforceps. Cut the loop pedicle at a distance of 1 cm from the chamber opening with dissecting scissors and remove the chamber.
11. Open the lid of the chamber and carefully remove the construct from the chamber with forceps and fix it in 4% buffered formalin solution for 24 hr at room temperature. Afterwards use the construct for 3D micro-computed tomography or paraffin-embedded for histological analysis<sup>30</sup>.

## Representative Results

### Tissue Engineering

For bone tissue engineering purposes, a number of different bone substitutes were implanted in the small animal rat AV loop model<sup>27,28,33,34</sup>. Vascularization could perfectly be demonstrated by 3D micro-computed tomography (micro-CT) (**Figure 3A**). Vascularization of a processed bovine cancellous bone (PBCB) matrix was significantly higher in the loop group compared to the group without vascularization. A constantly growing and maturing blood vessel network developed within the implantation chamber over 8 weeks. Between 4 and 8 weeks, continuous growth of the vascularized tissue towards the center of the constructs was observed, whereas no increase was detected in the non-vascularized group<sup>33</sup>. Prevascularization of the PBCB matrix for 6 weeks in the AV loop model led to superior survival of the injected osteoblasts compared to the control osteoblasts. In contrast to the control groups, expression of bone-specific genes was detected in the AV loop group with implanted osteoblasts<sup>28</sup>. As a further matrix, sintered bioactive glass together with fibrin gel was implanted in the AV loops of the rats. After 3 weeks, a dense network of newly formed vessels has developed demonstrated by micro-CT and histology<sup>27</sup>.

The implantation chamber was modified in order to accelerate scaffold vascularization. By using a perforated titanium chamber, intrinsic vascularization was supported by extrinsic vessels from the surrounding tissue. At just 2 weeks after implantation of a  $\beta$ -tricalciumphosphate hydroxyapatite ( $\beta$ -TCP/HA)/fibrin matrix, 83% of the vessels were connected to the AV loop with continuous increase over time and reached 97% connection after 8 weeks<sup>34</sup>. With the implantation of  $5 \times 10^6$  bone marrow derived mesenchymal stem cells (MSC) and bone morphogenetic protein 2 (BMP-2), a significant increase in bone formation compared to the BMP-2 or MSC alone groups could be induced. At 6 and 12 weeks, the fibrin matrix was completely degraded and replaced by highly vascularized connective tissue in all groups (**Figure 3B** 6 week implantation). There was a significant decrease in vessel number in the BMP-2/MSC group between 6 and 12 weeks and after 12 weeks in the other groups. This was probably due to maturation of the vascular network or the compact arrangement of bone structures leading to a limited vascular network formation<sup>32</sup>.

Besides bone, other tissues such as muscle or liver can also be engineered in the AV loop model.

For engineering axially vascularized muscle tissue, experiments with primary myoblasts in an AV loop fibrin matrix were carried out. After a prevascularization time of 2 weeks for 2, 4, and 8 weeks,  $1 \times 10^6$  myoblasts were transplanted into the AV loop chamber. Transplanted myoblasts could be redetected even after 8 weeks using carboxyfluorescein diacetate succinimidyl ester (CFDA) labeling. The cells kept their myogenic phenotype within the fibrin matrix and expression of the muscle-specific markers MEF-2 and desmin was positive after 4 weeks. However, myogenic marker gene expression was negative after 8 weeks, which was probably due to the absence of myogenic stimuli and rapid absorption of the fibrin matrix<sup>35</sup>. To increase myogenic stimulation, a new modification of the rat AV loop was developed using the epigastric vein instead of the saphenous vein in order to achieve a more proximal positioning of the isolation chamber. Hence, additional incorporation of the obturator motor nerve was geometrically facilitated. By using this AV loop modification, which is referred to as the EPI loop, we could show myogenic differentiation of co-implanted myoblasts and MSC<sup>36</sup>.

For hepatic tissue engineering  $4 \times 10^6$  pkh-26 labeled fetal liver cells were transplanted within a fibrin matrix in the rat AV loop model for 2 weeks. In the control group, matrices without an AV loop and cell-free matrices were implanted. Functional capillaries arose from the AV loop vessels and highly vascularized neo-tissue was observed within the chamber after 14 days of implantation, as shown by CD31 staining and India ink labeling. There was no difference between the cell-free and hepatocyte AV loop group. The AV loop vascularized the fibrin matrix densely and viable fetal cells could be detected after explantation by positive pkh-26 staining and liver cell-specific cytokeratin 18 (CK-18) immunohistology mainly in the proximity of the major vascular axis. mRNA levels of CK-18 were elevated in the AV loop cell group. In contrast, no CK-18 expression could be detected in constructs without a loop or cells<sup>37</sup>.

### Angiogenesis Studies

The AV loop consists of three segments: the vein, the arterial graft and the interpositional venous graft (IVG) segment (**Figure 1**). Three-dimensional evaluation of the vascular system demonstrated that newly formed vessels originated both from the venous and arterial portion as well as from the venous interponate. A great number of newly formed vessels were observed from the IVG<sup>33</sup>. With *in vivo* MRA, scanning electron microscopy of corrosion casts and immune histology, the onset of angiogenesis in a fibrin matrix was observed between day 10 and 14. Above all, the venous and IVG segments gave rise to many capillaries and larger vessels. A gradual reduction in luminal caliber as a sign of arterIALIZATION of the IVG due to the increase in endovascular pressure and shear stress was detected from day 7 on<sup>38</sup>. In further studies, it could be confirmed that vascular sprouting mainly takes place at the non-arterial graft<sup>39</sup>.

The exact analysis of angiogenesis processes and the stimulation and inhibition of blood vessel formation could be visualized in the AV loop implantation chamber. The growth factors vascular endothelial growth factor A (VEGFA) and basic fibroblast growth factor (bFGF) induced a higher absolute and relative vascular density and faster resorption of the fibrin matrix compared to the growth factor-free control group<sup>31</sup>. Further, remodeling phenomena and maturation of the vascular network within the isolation chamber were visualized over an implantation period of 8 weeks. In AV loop chambers processes of intercapillary interconnection and intussusceptive angiogenesis as well as possible lymphatic growth were identified immunohistologically as parameters of neovascular maturation<sup>39</sup>. By applying the PHD (prolyl hydroxylase domain) inhibitor DMOG (dimethyloxallyl glycine) systemically in rats, it could be shown that the concentration of the hypoxia-inducible factor alpha (HIF- $\alpha$ ) correlates with the growing vascularization in the AV loop and is a stimulus for vessel outgrowth<sup>40</sup>.



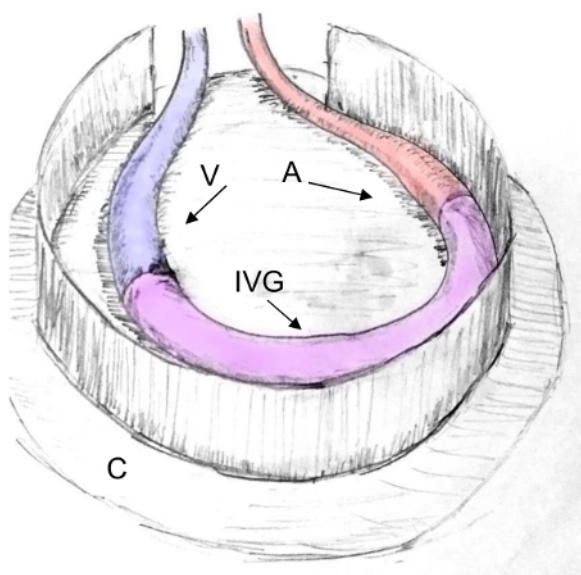


**Figure 1: Scheme of an AV Loop in the Rat Model.** The AV loop consists of three segments: the vein (V), the arterial (A) graft and the interpositional venous graft (IVG) segment. The AV loop can be embedded into a closed implantation chamber (C) for induction of intrinsic vascularization. [Please click here to view a larger version of this figure.](#)

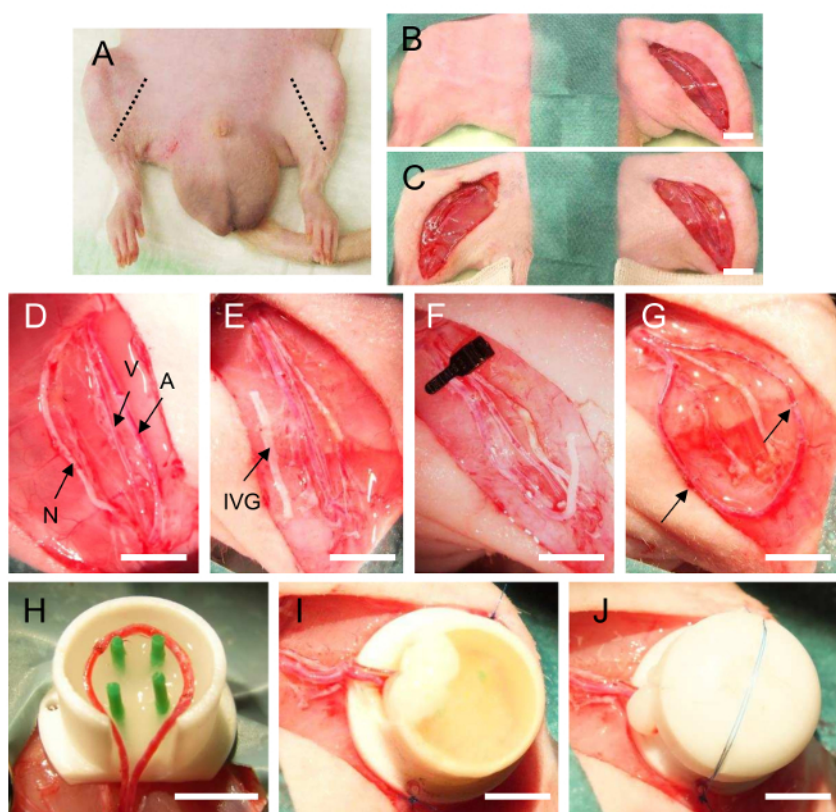


**Figure 2: AV Loop Operation in the Rat.** (A): Localization of the femoral bundle on the inner side of the hind limbs of the rat. (B/C): Preparation of the femoral vascular bundle in the left and right groin of the rat. The vessels are separated (D), the interpositional vein graft is harvested from the right side (E) and anastomosed with the femoral vein (F) and femoral artery of the left side into an AV loop (G, arrow indicates the anastomoses). The loop vessels are transferred into the implantation chamber prefilled with a matrix (H) and after complete filling (I) the lid is closed (J). A = femoral artery, V = femoral vein, N = femoral nerve, IVG = interpositional venous graft. Scale bar 5 mm (D-J). [Please click here to view a larger version of this figure.](#)

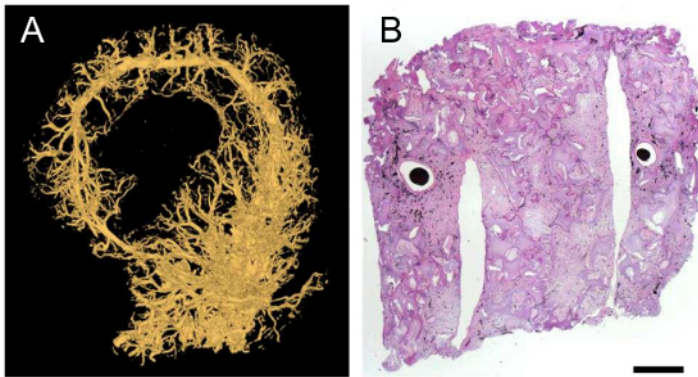


**Figure 3: Visualization of Vascularization in the Rat AV Loop Model.** (A): Micro-CT after perfusion with a contrast agent (yellow perfused vessels). (B): Hematoxylin-Eosin staining of a  $\beta$ -TCP/HA bone substitute with MSC implanted in the AV loop model rat for 6 weeks. The AV loop vessels are perfused with India ink (black color). Scale bar 1 mm. [Please click here to view a larger version of this figure.](#)

## Discussion

For over a decade, we have successfully used the arteriovenous (AV) loop for tissue engineering purposes and studying angiogenesis *in vivo* in the small animal model. We could demonstrate that this microsurgical model is very well suited for engineering different tissues and that it can also be used for angiogenesis or antiangiogenesis studies.

### Significance of the Technique with Respect to Existing/Alternative Methods

Engineered tissues or organs require a functional blood vessel network to supply the nutrients and oxygen they need for their survival and successful integration after transplantation into the defect site<sup>41</sup>. A number of different prevascularization strategies have been developed over the past decades, which can be differentiated according to *in vitro* vs. *in vivo* and extrinsic vs. intrinsic approaches.

Scaffolds can be fabricated with tubular-shaped structures and seeded with vascular cells such as endothelial cells or progenitor cells *in vitro*<sup>42</sup>. On the other hand, for *in vivo* prevascularization, scaffolds are implanted in a highly vascularized area such as subcutaneous or muscle tissue<sup>21</sup>. Afterwards, these extrinsically vascularized constructs can be transplanted into the defect site. However, the drawback of these approaches is the lack of microsurgical connection with the recipient's vessels after transplantation. Particularly in the case of large-scale constructs, immediate connection to the host vasculature is essential for immediate supply of the engineered tissue<sup>43</sup>. The obvious and most promising solution to this problem lies in the generation of an intrinsically vascularized tissue or organ by a vascular axis, such as the AV loop model.

Besides using the AV loop method as described above, axial vascularization can also be induced by using AV bundles instead<sup>44</sup> or only one vessel such as the epigastric artery<sup>45</sup>. However, in several publications the AV loop model proved to be superior with regard to degree of vascularization and the amount of *de novo* tissue formation. Tanaka *et al.* compared both methodological approaches and observed significantly higher tissue formation and a greater degree of developing capillaries in the loop compared to the bundle group<sup>46</sup>. Dong *et al.* also conducted a study using the AV loop or AV bundle approaches for bone tissue engineering in a rabbit model, which likewise showed significantly higher vascular density in the loop compared to the bundle group<sup>47</sup>. We were able to confirm these results as well as show in a previous study that the AV loop model has a higher capacity for angiogenesis<sup>48</sup>.

To the best of our knowledge, there is no comparable model for analyzing vascularization *in vivo* in an isolated and well-characterized environment. Therefore, the AV loop model represents a powerful tool for evaluating how different cell types or growth factors contribute to vessel network formation or vascularization processes in different tissues without disturbances from surrounding structures, such as invading cells or growth factors.

### Limitations of the Technique

However, one significant challenge of the proposed model is the high complexity of the surgery. For one, the treatment of defects using the AV loop model requires a two-step procedure - prevascularization of the scaffold and transplantation into the defect site. This means that the patient has to undergo two surgeries. In addition, microsurgical skills are a necessary prerequisite for successful anastomosing submillimeter vessels<sup>49</sup>. Therefore, the AV bundle is sometimes considered more useful for clinical application since it also offers promising, although less, potential for angiogenesis and tissue generation compared to the AV loop<sup>46</sup>. However, this operation can be learned step-by-step even by non-surgeons, using small caliber silicon tubes for the training in the beginning and afterwards the vessels of dead animals (e.g., chicken legs) before doing the AV loop operation in a live animal. In contrast, most practiced micro-surgeons can perform this operation with only a short time of training.

### Critical Steps within the Protocol

In general, due to the small caliber of the vessels there is the risk of thrombus formation and closure of the loop vessels. However, in the rat model 80%-100% of the loops on average were patent using only short-time heparin anticoagulation post-surgery<sup>28,30,31,34,38,39</sup>.

Furthermore, due to the high complexity of the surgery it will take a couple of hours (depending on the expertise of the surgeon). It is essential to check proper anesthesia of animals during the whole operation and to adequately supply infusion for maintaining an adequate blood pressure. During the postoperative period it is of high importance to check the health of the animal several times, to administer analgesics/antibiotics and to check the operation wound. Since in most cases implantation of an isolated chamber is performed, it is possible that infection in the inner

of the chamber occurs without noticing. Therefore, it is very important to maintain sterility during the whole operation and administration of antibiotics should carefully be done over a period of 3 - 5 days.

### Modifications of the Protocol

The chamber can be individually adjusted to the size and shape of the defect. Furthermore, also membranes can be used for enclosing the AV loop as performed by Manasseri *et al.*<sup>50</sup>. In addition, the scaffold, supplemented cells and growth factors can be chosen according to the different tissue types. Recently, Miomas *et al.* combined gene therapeutic approaches successfully with the AV loop model and could induce enhancement of vessel growth by transduction with VEGF165<sup>51</sup>. Recently, we adjusted the rat AV loop model for muscle tissue engineering purposes. Instead of the femoral vessels, the epigastric vein and saphenous artery were used, which enabled implantation of the obturator nerve in the axially vascularized scaffold for motoric innervation ("EPI loop model")<sup>36</sup>. Besides implantation of a motoric nerve, the neurotization of bone tissue engineered constructs with sensory nerves is reported to be beneficial for enhanced osteogenesis and better repair of bone defects<sup>52</sup>. The AV loop induces minimal donor site morbidity and can be created at various sites of the body<sup>52</sup>. It would be possible to use superficial vessels at other sites of the body for generation of the AV loop or even to use other animals such as the rabbit or the mouse model.

### Future Applications or Directions after Mastering this Technique

Recently, our working group implanted a well-characterized murine embryonal endothelial progenitor cell (EPC) line (T17b) expressing the guanylate binding protein-1 (GBP-1) - a marker and intracellular inhibitor of endothelial cell functions such as proliferation, migration and invasion - in the rat AV loop model. The antiangiogenic capacity of differentiated GBP-1-EPC could be demonstrated by a significant reduction of blood vessel density in the AV loop constructs. With regard to clinical application, the proinflammatory antiangiogenic GTPase GBP-1 could open up new avenues of antiangiogenic therapies, e.g., for cancer or other diseases<sup>53</sup>. Based on this study, it is conceivable that the AV loop model can be used for establishing a pathological vascularization network for further analysis and possible modulation. For example, this model provides an optimal opportunity to gain a better understanding of tumor angiogenesis, its influencing factors and the exact role of the different cells involved in tumor vessel network formation such as EPCs, tumor cells and stem cells<sup>54</sup>. *In vivo* cancer models are often carried out in genetically modified mice to simulate the processes and growth characteristics of different human cancer types and have proven to be excellent for drug development and preclinical trials<sup>55</sup>. Furthermore, there are xenograft models for transplanting tumors into experimental animals such as immunocompromised mice<sup>56</sup>. A more clinically related approach involves transplantation from the patient's tumor, known as "personalized mouse models" or "patient-derived tumor xenografts models"<sup>57</sup>. However, these models are not practical for studying the influence of one single cell source or growth factor without effects from the surrounding tissue.

The AV loop model makes it possible to use tissue engineering methods to study tumor biology. This is defined as "tumor engineering" by Ghajar *et al.* and involves "the construction of complex culture models that recapitulate aspects of the *in vivo* tumor microenvironment to study the dynamics of tumor development, progression, and therapy on multiple scales"<sup>58</sup>. A tumor environment can be constructed within the isolated implantation chamber, which allows a precise analysis of cell-cell interactions, angiogenesis, modulation, enhancement and inhibition. Furthermore, the AV loop model may prove beneficial for developing or validating therapies concerning the interruption of neoangiogenesis or the inhibition of tumor growth.

Using this approach for inducing vascularization, it is possible to engineer tissues in a clinically relevant size. In further studies, we were able to generate axially vascularized bone tissue for transplantation with a significant volume of about 15 cm<sup>3</sup> in a relatively short time of 12 weeks<sup>59,60</sup>. In order to translate these findings to clinical practice, a proof of principle study using the tibia defect model will be performed in the near future prior for application in humans. As a first step, we could successfully demonstrate *in situ* bone tissue engineering in a large volume defect in a clinical scenario with long-term stability<sup>61</sup>. Applying the described AV loop model makes it is possible to provide a therapy tailored to the individual patient's requirements. Based on our results the idea of the human body itself serving as a living bioreactor still holds great promise for the future.

## Disclosures

The authors have nothing to disclose.

## Acknowledgements

We would like to thank the following institutions for supporting our AV loop research: Staedtler Stiftung, Dr. Fritz Erler Fonds, Else Kröner Fesenius Stiftung, Baxter Healthcare GmbH, DFG, IZKF/ELAN/EFI/Office for Gender and Diversity, the Forschungsstiftung Medizin, Friedrich-Alexander University of Erlangen-Nürnberg (FAU), AO Foundation, Manfred Roth Stiftung, Xue Hong, Hans Georg Geis Foundation, Deutscher Akademischer Austauschdienst (DAAD), Germany, and the Ministry of Higher Education and Scientific Research, Iraq. We would like to thank Stefan Fleischer, Marina Milde, Katrin Köhn and Ilse Arnold-Herberth for their excellent technical support.

## References

1. Folkman, J., & Haudenschild, C. Angiogenesis in vitro. *Nature*. **288** (5791), 551-556 (1980).
2. DeCicco-Skinner, K. L. *et al.* Endothelial cell tube formation assay for the in vitro study of angiogenesis. *J Vis Exp.* (91), e51312 (2014).
3. Puddu, A., Sanguineti, R., Traverso, C. E., Viviani, G. L., & Nicolo, M. Response to anti-VEGF-A treatment of endothelial cells in vitro. *Exp Eye Res.* **146** 128-136 (2016).
4. Li, H., Daculsi, R., Bareille, R., Bourget, C., & Amedee, J. uPA and MMP-2 were involved in self-assembled network formation in a two dimensional co-culture model of bone marrow stromal cells and endothelial cells. *J Cell Biochem.* **114** (3), 650-657 (2013).
5. Griffith, L. G., & Swartz, M. A. Capturing complex 3D tissue physiology in vitro. *Nat Rev Mol Cell Biol.* **7** (3), 211-224 (2006).
6. Nehls, V., & Herrmann, R. The configuration of fibrin clots determines capillary morphogenesis and endothelial cell migration. *Microvasc Res.* **51** (3), 347-364 (1996).



7. Fischbach, C. *et al.* Cancer cell angiogenic capability is regulated by 3D culture and integrin engagement. *Proc Natl Acad Sci U S A.* **106** (2), 399-404 (2009).
8. Logsdon, E. A., Finley, S. D., Popel, A. S., & Mac Gabhann, F. A systems biology view of blood vessel growth and remodelling. *J Cell Mol Med.* **18** (8), 1491-1508 (2014).
9. Kaully, T., Kaufman-Francis, K., Lesman, A., & Levenberg, S. Vascularization—the conduit to viable engineered tissues. *Tissue Eng Part B Rev.* **15** (2), 159-169 (2009).
10. Risau, W. Mechanisms of angiogenesis. *Nature.* **386** (6626), 671-674 (1997).
11. Carmeliet, P. Mechanisms of angiogenesis and arteriogenesis. *Nat Med.* **6** (4), 389-395 (2000).
12. Morin, K. T., & Tranquillo, R. T. In vitro models of angiogenesis and vasculogenesis in fibrin gel. *Exp Cell Res.* **319** (16), 2409-2417 (2013).
13. Ucuzian, A. A., & Greisler, H. P. In vitro models of angiogenesis. *World J Surg.* **31** (4), 654-663 (2007).
14. Staton, C. A., Reed, M. W., & Brown, N. J. A critical analysis of current in vitro and in vivo angiogenesis assays. *Int J Exp Pathol.* **90** (3), 195-221 (2009).
15. Tahergorabi, Z., & Khazaei, M. A review on angiogenesis and its assays. *Iran J Basic Med Sci.* **15** (6), 1110-1126 (2012).
16. Agostini, S. *et al.* Barley beta-glucan promotes MnSOD expression and enhances angiogenesis under oxidative microenvironment. *J Cell Mol Med.* **19** (1), 227-238 (2015).
17. Zhang, B., Xuan, C., Ji, Y., Zhang, W., & Wang, D. Zebrafish xenotransplantation as a tool for in vivo cancer study. *Fam Cancer.* **14** (3), 487-493 (2015).
18. Devaud, C. *et al.* Tissues in different anatomical sites can sculpt and vary the tumor microenvironment to affect responses to therapy. *Mol Ther.* **22** (1), 18-27 (2014).
19. Min, Z., Shichang, Z., Chen, X., Yufang, Z., & Changqing, Z. 3D-printed dimethylallyl glycine delivery scaffolds to improve angiogenesis and osteogenesis. *Biomater Sci.* **3** (8), 1236-1244 (2015).
20. Sundaram, S. *et al.* Tissue-engineered vascular grafts created from human induced pluripotent stem cells. *Stem Cells Transl Med.* **3** (12), 1535-1543 (2014).
21. Hori, A., Agata, H., Takaoka, M., Tojo, A., & Kagami, H. Effect of Cell Seeding Conditions on the Efficiency of In Vivo Bone Formation. *Int J Oral Maxillofac Implants.* **31** (1), 232-239 (2016).
22. Laschke, M. W., & Menger, M. D. Prevascularization in tissue engineering: Current concepts and future directions. *Biotechnol Adv.* (2015).
23. Wong, H. K. *et al.* Novel method to improve vascularization of tissue engineered constructs with biodegradable fibers. *Biofabrication.* **8** (1), 015004 (2016).
24. Rouwkema, J., de Boer, J., & Van Blitterswijk, C. A. Endothelial cells assemble into a 3-dimensional prevascular network in a bone tissue engineering construct. *Tissue Eng.* **12** (9), 2685-2693 (2006).
25. Lokmic, Z., & Mitchell, G. M. Engineering the microcirculation. *Tissue Eng Part B Rev.* **14** (1), 87-103 (2008).
26. Erol, O. O., & Spira, M. New capillary bed formation with a surgically constructed arteriovenous fistula. *Surg Forum.* **30** 530-531 (1979).
27. Arkudas, A. *et al.* Evaluation of angiogenesis of bioactive glass in the arteriovenous loop model. *Tissue Eng Part C Methods.* **19** (6), 479-486 (2013).
28. Arkudas, A. *et al.* Axial prevascularization of porous matrices using an arteriovenous loop promotes survival and differentiation of transplanted autologous osteoblasts. *Tissue Eng.* **13** (7), 1549-1560 (2007).
29. Arkudas, A. *et al.* Composition of fibrin glues significantly influences axial vascularization and degradation in isolation chamber model. *Blood Coagul Fibrinolysis.* **23** (5), 419-427 (2012).
30. Arkudas, A. *et al.* Dose-finding study of fibrin gel-immobilized vascular endothelial growth factor 165 and basic fibroblast growth factor in the arteriovenous loop rat model. *Tissue Eng Part A.* **15** (9), 2501-2511 (2009).
31. Arkudas, A. *et al.* Fibrin gel-immobilized VEGF and bFGF efficiently stimulate angiogenesis in the AV loop model. *Mol Med.* **13** (9-10), 480-487 (2007).
32. Buehrer, G. *et al.* Combination of BMP2 and MSCs significantly increases bone formation in the rat arterio-venous loop model. *Tissue Eng Part A.* **21** (1-2), 96-105 (2015).
33. Kneser, U. *et al.* Engineering of vascularized transplantable bone tissues: induction of axial vascularization in an osteoconductive matrix using an arteriovenous loop. *Tissue Eng.* **12** (7), 1721-1731 (2006).
34. Arkudas, A. *et al.* Combination of extrinsic and intrinsic pathways significantly accelerates axial vascularization of bioartificial tissues. *Plast Reconstr Surg.* **129** (1), 55e-65e (2012).
35. Bach, A. D. *et al.* A new approach to tissue engineering of vascularized skeletal muscle. *J Cell Mol Med.* **10** (3), 716-726 (2006).
36. Bitto, F. F. *et al.* Myogenic differentiation of mesenchymal stem cells in a newly developed neurotised AV-loop model. *Biomed Res Int.* **2013** 935046 (2013).
37. Fiegel, H. C. *et al.* Foetal hepatocyte transplantation in a vascularized AV-Loop transplantation model in the rat. *J Cell Mol Med.* **14** (1-2), 267-274 (2010).
38. Polykandriotis, E. *et al.* The venous graft as an effector of early angiogenesis in a fibrin matrix. *Microvasc Res.* **75** (1), 25-33 (2008).
39. Polykandriotis, E. *et al.* Regression and persistence: remodelling in a tissue engineered axial vascular assembly. *J Cell Mol Med.* **13** (10), 4166-4175 (2009).
40. Yuan, Q. *et al.* PHDs inhibitor DMOG promotes the vascularization process in the AV loop by HIF-1 $\alpha$  up-regulation and the preliminary discussion on its kinetics in rat. *BMC Biotechnol.* **14** 112 (2014).
41. Dew, L., MacNeil, S., & Chong, C. K. Vascularization strategies for tissue engineers. *Regen Med.* **10** (2), 211-224 (2015).
42. Kang, Y., Mochizuki, N., Khademhosseini, A., Fukuda, J., & Yang, Y. Engineering a vascularized collagen-beta-tricalcium phosphate graft using an electrochemical approach. *Acta Biomater.* **11** 449-458 (2015).
43. Novosel, E. C., Kleinhans, C., & Kluger, P. J. Vascularization is the key challenge in tissue engineering. *Adv Drug Deliv Rev.* **63** (4-5), 300-311 (2011).
44. Zimmerer, R., Jehn, P., Spalthoff, S., Kokemuller, H., & Gellrich, N. C. [Prefabrication of vascularized facial bones]. *Chirurg.* **86** (3), 254-258 (2015).
45. Dunda, S. E. *et al.* [In Vitro and In Vivo Biocompatibility of a Novel, 3-Dimensional Cellulose Matrix Structure]. *Handchir Mikrochir Plast Chir.* **47** (6), 378-383 (2015).
46. Tanaka, Y. *et al.* Tissue engineering skin flaps: which vascular carrier, arteriovenous shunt loop or arteriovenous bundle, has more potential for angiogenesis and tissue generation? *Plast Reconstr Surg.* **112** (6), 1636-1644 (2003).



47. Dong, Q. S. *et al.* Prefabrication of axial vascularized tissue engineering coral bone by an arteriovenous loop: a better model. *Mater Sci Eng C Mater Biol Appl.* **32** (6), 1536-1541 (2012).
48. Polykandriotis, E. *et al.* [Prevascularisation strategies in tissue engineering]. *Handchir Mikrochir Plast Chir.* **38** (4), 217-223 (2006).
49. Mofikoya, B. O., Ugburo, A. O., & Bankole, O. B. Does open guide suture technique improve the patency rate in submillimeter rat artery anastomosis? *Handchir Mikrochir Plast Chir.* **46** (2), 105-107 (2014).
50. Manasseri, B. *et al.* Microsurgical arteriovenous loops and biological templates: a novel in vivo chamber for tissue engineering. *Microsurgery.* **27** (7), 623-629 (2007).
51. Moimas, S. *et al.* AAV vector encoding human VEGF165-transduced pectineus muscular flaps increase the formation of new tissue through induction of angiogenesis in an in vivo chamber for tissue engineering: A technique to enhance tissue and vessels in microsurgically engineered tissue. *J Tissue Eng.* **6** 2041731415611717 (2015).
52. Fan, J. *et al.* Microsurgical techniques used to construct the vascularized and neurotized tissue engineered bone. *Biomed Res Int.* **2014** 281872 (2014).
53. Bleiziffer, O. *et al.* Guanylate-binding protein 1 expression from embryonal endothelial progenitor cells reduces blood vessel density and cellular apoptosis in an axially vascularised tissue-engineered construct. *BMC Biotechnol.* **12** 94 (2012).
54. Horch, R. E. *et al.* Cancer research by means of tissue engineering--is there a rationale? *J Cell Mol Med.* **17** (10), 1197-1206 (2013).
55. Lee, H. Genetically engineered mouse models for drug development and preclinical trials. *Biomol Ther (Seoul).* **22** (4), 267-274 (2014).
56. Willey, C. D., Gilbert, A. N., Anderson, J. C., & Gillespie, G. Y. Patient-Derived Xenografts as a Model System for Radiation Research. *Semin Radiat Oncol.* **25** (4), 273-280 (2015).
57. Guirao, K., & Arinzeh, T. L. Bioengineering Models for Breast Cancer Research. *Breast Cancer (Auckl).* **9** (Suppl 2), 57-70 (2015).
58. Ghajar, C. M., & Bissell, M. J. Tumor engineering: the other face of tissue engineering. *Tissue Eng Part A.* **16** (7), 2153-2156 (2010).
59. Boos, A. M. *et al.* Engineering axially vascularized bone in the sheep arteriovenous-loop model. *J Tissue Eng Regen Med.* **7** (8), 654-664 (2013).
60. Weigand, A. *et al.* Acceleration of vascularized bone tissue-engineered constructs in a large animal model combining intrinsic and extrinsic vascularization. *Tissue Eng Part A.* **21** (9-10), 1680-1694 (2015).
61. Horch, R. E., Beier, J. P., Kneser, U., & Arkudas, A. Successful human long-term application of in situ bone tissue engineering. *J Cell Mol Med.* **18** (7), 1478-1485 (2014).